Journal of Applied Surfaces and Interfaces 5(1-3) (2019) 21-30

Journal homepage:http://revues.imist.ma/?journal=jasi

ISSN: 2550-4800

https://doi.org/10.48442/IMIST.PRSM/jasi-v5i1-3.17459

JASI JOURNAL OF APPLIED SURFACES AND INTERFACES

Simultaneous adsorption of mercury (II) and zinc (II) ions from aqueous solution onto activated carbons derived from a lowland bioresource waste

Peter P. Ndibewu[1], Charles M. Kede[1,2,], Pierre G. Tchieta[1], Harlette Z. Poumve[1], Armand N. Tchakounte[1].*

[1]*Department of Chemistry, Faculty of Science, Tshwane University of Technology, P. O. Box 56208, 0007 Arcadia, Pretoria, Republic of S. Africa.*
[2]*Department of Chemistry, Faculty of Science, University of Douala, P.O. Box 24175, Douala, Cameroon.*

Received 15 August 2019; Revised 18 October 2019; Accepted 20 October 2019.

Abstract: *Adsorption of Hg(II) and Zn(II) ions from a binary solution was examined using activated carbons (ACs) prepared from a lowland bioresource waste (Theobroma cacao pod husk). The aim of the study was to determine the potential for utilizing the plant-based ACs as a low-cost adsorbent for removing the metal ions from a binary. Batch adsorption experimentations were conducted to evaluate the initial metal ion concentration and contact time on adsorption. Spectroscopic studies including FTIR, elemental analysis (EA) and SEM were used for its characterization. Equilibrium data was examined using a comparison of linear Langmuir, Freundlich and Temkin isotherm models. The Langmuir and Temkin isotherm model provided the best fit to the experimental data for both metal ions as indicated by the values of the regression coefficient. The kinetic rates were modeled by using the Lagergren-first-order, pseudo-second-order, Elovich and Intraparticle model. The pseudo-first order, pseudo-second order equations and Elovich equation gave the best fit to the experimental data. The presence of intra-particle diffusion mechanism was prominent, although it was not the sole rate-determining step. The results showed that ACs can be effective for removing Hg(II) and Zn(II) ions from solution.*

Keywords: *Mercury; Zinc; Adsorption; Activated carbons; Bioresource waste; Theobroma cacao pod husk.*

1. Introduction

The increasing discharge of industrial wastewaters containing heavy metals into the environment has been on the increase because of rapid growth of industries. This is a serious problem because heavy metals at high concentrations are toxic to aquatic eco-systems causing harmful effects to organisms living in both the marine and fresh water environments, plants and the humans [1].

Mercury has no beneficial biological function and its presence in living organisms is associated with cancer, birth defects and other undesirable outcomes [2]. Mercury enters the human body mainly through seafood, drinking water and inhalation of polluted air [3]. According to the United States Environmental Protection Agency (USEPA), the tolerance limit for Hg^{2+} for drinking water is 1µg/L [4,5]. Hg(II) causes damage to the central nervous system and chromosomes, impairment of pulmonary function and kidneys, chest pain and dyspnea [4]. The main sources of zinc in wastewater are anthropogenic [3]. This include wastes discharge streams from metals, chemicals, pulp and paper manufacturing processes, steel works with galvanizing lines, zinc and brass metal works, zinc and brass plating, viscose rayon yarn and fiber production [6]. The World Health Organization recommended the maximum acceptable concentration of zinc in drinking water as 3.0 mg/L [7].

Conventional methods for removing Hg(II) and Zn(II) from aqueous solutions include sulphide precipitation, ion exchange, alum and iron coagulation and reverse osmosis [8]. However, Hg^{2+} and Zn^{2+} removal costs for most of these methods are still very high. This has led to the intensification of research focused on new materials and technologies that will provide for an effective and economic removal of Hg(II) and Zn(II) from aqueous solutions. Recent developments has been on the investigation of non-conventional adsorbents like activated carbons from agricultural and food wastes [9], bentonite [10], modified forms of palm shell [11], and natural and aluminum pillared clays [12] reported to be used with success to some extent for the removal of Hg(II) from aqueous solutions including waste Fe(III)/Cr(III) hydroxide.

Besides the economic implications, the use of agricultural by-products has many environmental benefits [13,14]. In the cocoa producing regions of the world (e.g. Cameroon, Cote d'Ivoire and Ghana in Africa and Brazil in the Amazon), agricultural wastes such as Theobroma cocoa pod husk are often disposed of under unsuitable conditions. These then rot generating bad smells (unhygienic) with considerable negative impacts on the landscape or provide favorable environments for microorganisms to flourish which eventually find their way into drinking water streams. It is postulated that the use of activated carbons from Theobroma cocoa

* *Corresponding author: E-mail: meleack@yahoo.fr (Charles M. Kede)*

pod husk can effectively remove Hg(II) and Zn(II) from aqueous solutions. Advantages linked to the use of this kind of agricultural waste are very rewarding. Firstly, its use would add value to an agricultural by-product since it is disposed of as a waste. Secondly, the importance of effective and economic removal of Hg(II) and Zn(II)cannot be overemphasized here, as it is global problem. Thirdly and finally, Theobroma cocoa pod husk is considered a renewable resource because it can be replenished continuously.

Cocoa pod husk represents between 70 to 75 % of the whole mass of the cocoa fruit, i.e. 700 to 750 kg of waste can be generated from a ton of cocoa fruit. Nevertheless, various techniques have been developed as alternative methods of disposal while creating valuable products, e.g. food antioxidants [15], dietary fibers [16], and animal feed [17]. Cocoa pod husk possesses suitable characteristics making it a good precursor for the preparation of activated carbons owing to its cellulosic (41.92%) and hemicellulosic content [18].

Kadirvelu et al. reported from a preliminary finding that carbonized Theobroma cacao pod husk is effective for the treatment of dyeing wastewater and for removing of As, Cd, Cu, Cr, Hg and Ni ions from solution [19]. Other authors have also reported the successful removal of organics, including pesticides from aqueous solutions [20-22].

The objective of this study was to investigate the feasibility of using carbonized Theobroma cacao pod husk for the removal of Hg(II) and Zn(II) from wastewater by adsorption.

2. Materials and methods

2.1. Reagents and materials

All the chemicals used in the present work were of analytical reagent grade obtained from Aldrich Chemical Co. Deionized doubly distilled (DDD) water was used throughout the experimental studies. Mercury and Zinc standard solutions (1000mg/L, Atomic Spectroscopy Standard, PerkinElmer, Inc, U.SA) were prepared by diluting 10 mg/L in a volume of 500 mL deionized water. Working standardswere prepared by progressive dilution of the mercury and zinc stock solution with DDD water.

The Theobroma cacao pod husks were obtained from a farm in Mbele (Cameroon, 4°10’0.02’’N and 11°32’00’’E). They were filtered through Whatman paper #4 (USA) to remove suspended particles and then stored in a laboratory fridge at 4°C until analysis.

2.2. Preparation of activated carbon

The preparation of activated carbon was carried out according to the procedure recommended by Kede et al. [23]. The solid residue of Theobroma cacao was manually chosen; cleaned with deionized water, dried at 100°C for 24 hours, ground and passed through a sieve to obtain samples of 1-2.5 mm particle size. This raw material was treated with $ZnCl_2$ and $ZnCl_2/FeCl_3$ at two different concentrations (50 and 75%, m/m), ($ZnCl_2$, $ZnCl_2/FeCl_3$ solution/char, m/m) and pyrolysed in a tubular oven (Lindberg Blue), at three different temperatures (350, 450 and 550°C). These ratios were selected from previous investigations [24], which showed that the adsorption capacity increases remarkably with increasing $ZnCl_2$/char ratio. After the activation, the excess $ZnCl_2$ and $ZnCl_2/FeCl_3$were removed with a 0.1 M solution of hydrochloric acid (HCl), and then the product was washed with hot distilled water until a neutral pH was reached to obtain the sample for sorption measurements.

2.3. Characterization of activated carbons

The prepared activated carbons (ACs) from Theobroma cacao pod husk were examined with a scanning electron microscope (SEM) coupled to an X-ray (EDX) analyzer. N_2adsorption isotherms for pore size distribution (PSD) and surface areawere conducted with a Micromeritics ASAP 2010 (USA) surface area and porosity analyzer. Analyses of adsorption and desorption of nitrogen were conducted at 195°C. Before the experiments, the sample was degassed at 200°c overnight. Total surface areas were evaluated from the BET equation [25]. External surface areas were determined by applying the t-plot model between the range 7-9 Å [26]. Pore size distributions were determined using both BJH methods.

The surface structure of activated carbons was analyzed by Field emission scanning electron microscopy (FE-SEM) and energy-dispersive X-ray (EDX). The samples were gold coated to improve their conductivity to obtain good images. Elemental analysis (EA) for the carbon (C), nitrogen (N), oxygen (O), sulphur (S) and metal content of the various samples was carried out with the aid of the energy dispersive-X-ray device. The instrument used to obtain SEM images of the samples and EDS spectra was a JEOL JSM-7600F field emission scanning electron microscope, 800 mm^2, X-Max coupled to a silicon drift energy dispersive X-ray detector (SDD) (Oxford Instruments Ltd, UK).

2.4. Adsorption studies

Adsorption experiments were carried out according to the procedure described in Fig.1.

3. Results and discussion

3.1. Characterization of activated carbons

In this work, one untreated Theobroma cacao pod husk sample (GAC_0) and three activated carbons were obtained as follows: (1) GAC_8: T= 550°C, 75% Zn for 3h), (2) GAC_1 (T = 450°C, 50% Zn for 3h), and (3) GAC_7 (T = 550°C, 50% Zn/Fe for 3h) via microwave induced 50 and 75% (w/w) of $ZnCl_2$ and $FeCl_3$ activation.

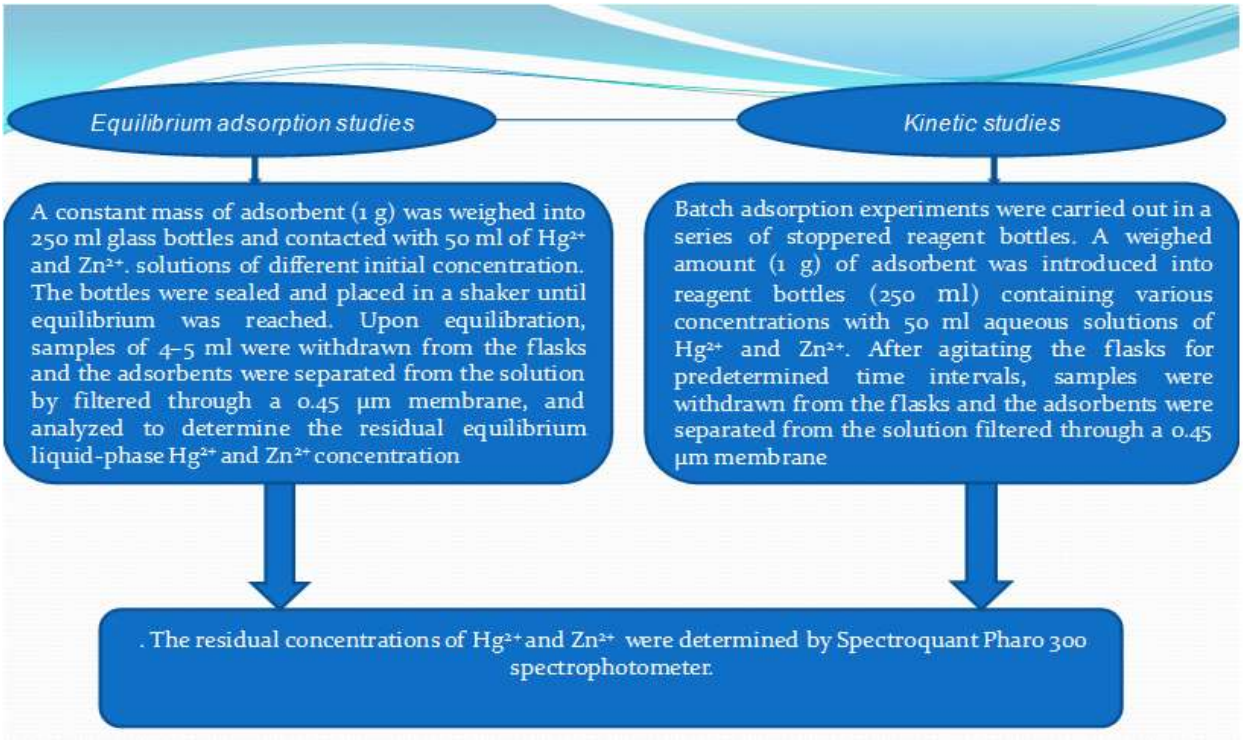

Fig.1.*An outline of the batch adsorption experimentations undertaken.*

3.1.1. Surface areas and pore sizes measurement

The N_2-adsorption isotherms at 77K for activated carbons produced from the Theobroma Cocoa by chemical activation are presented in Fig.2. All the samples gave type II isotherms, characteristic of micropores. The adsorption isotherms show adsorption-desorption hysteresis, indicating the presence of mesopores. Besides contributing significantly to the adsorption of the adsorbate, occurrence of the mesopores could be attributed to the interaction of functional groups at the surface of char which favors the evolution of molecules during the heating process of activation, then probably creating external pores [27]. The overall porosity development determined by N_2-adsorption at 77K using BET and BJH methods are shown in Table 1. From the table, it can be seen that all the samples have surface area between 357.36 and 586.93 m^2/g with highly developed microporosity.

3.1.2. Functionalization

The Fourier transform infrared (FTIR) spectra of the activated carbons are shown in Fig.3. The absorption at 2958 cm^{-1} indicates the presence of C-H groups [28]. The peaks appearing at 1542.1 and 1504.6 cm^{-1} are as a result of carbonyl groups (C=O) while the bands appearing at 1057.7, 1128.7 and 1162 cm^{-1} are ascribed to the formation of sulfur functional groups like a highly conjugated S=O.

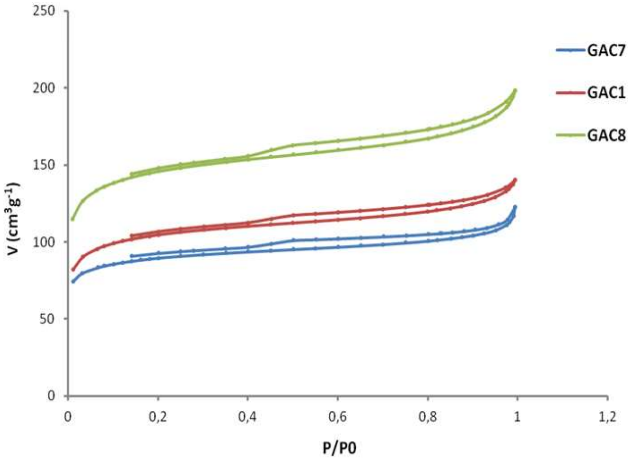

Fig.2*. N_2 adsorption/desorption isotherms for Theobroma cacao pod husk ACs*

Table 1

Characteristics of the Theobroma cacao pod husk activated carbons.

ACs	S_{BET} (m^2/g)	S_L (m^2/g)	S_{BJH} (m^2/g)	V_{TOTAL}(cm^3/g)	V_{BJH}(cm^3/g)	S_{BJH}/S_{BET}	D_{BET} (Å)
GAC_1	457.35	512.32	69.327	0.102	0.083	0.151	24.931
GAC_7	357.36	446.76	54.235	0.109	64.678	0.152	21.068
GAC_8	586.93	777.37	133.614	0.155	0.143	0.227	42.807

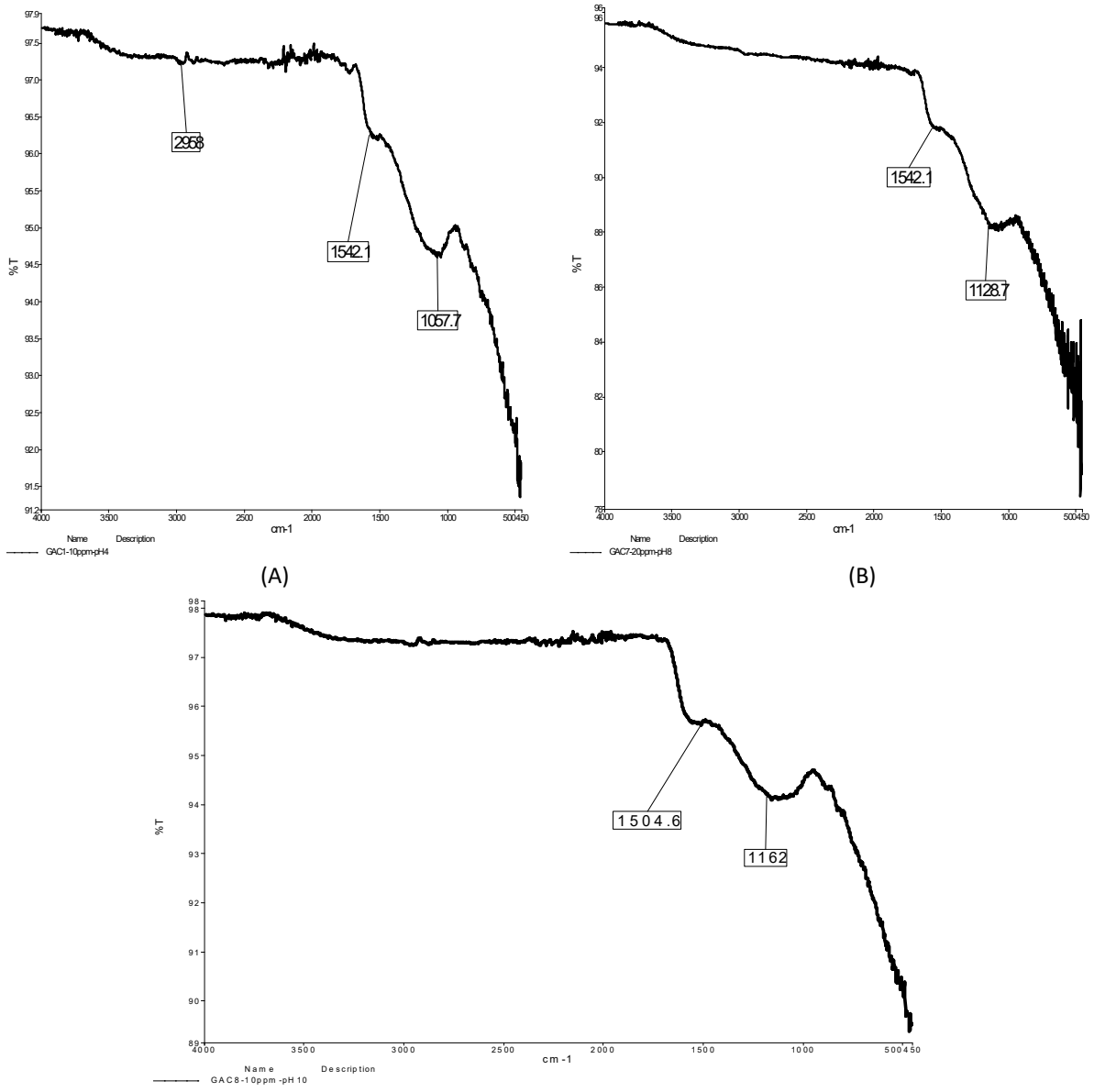

***Fig.3**. FTIR spectra for GAC_1 (A), GAC_7 (B) and GAC_8 (C)*

3.1.3. Surface morphology

To observe the morphology of the prepared AC samples, SEM images are shown in Fig.4. Fig.4a shows the micrograph for Theobroma cacao pod husk employed as the raw material for the preparation of the activated carbons. On one hand, the material presents a surface morphology in the form of plates, possibly with a low specific surface area. On the other hand, the micrographs shown in Figs.4b-d correspond to the materials collected after the activation process with $ZnCl_2$ and $FeCl_3$, with the salt mixture of 50%Zn, 75%Zn and 75%Zn/Fe, respectively, for GAC_1, GAC_8 and GAC_7, respectively. These images show that the morphology of the samples has changed after the activation process; suggesting that surface craters were produced, which contributes to the increase of the surface area after the activation. From this analysis, it is clear that the presence of zinc and iron species in the preparation of the samples produces "craters" with thinner walls on the surfaces thereby creating a weaker structure.

3.2. Adsorption studies

For the practical phase of the simultaneous adsorption of Hg(II) and Zn(II) ions the adsorbent with the greatest specific surface area (GAC_8) was used.

3.2.1. Effect of contact time of Hg(II) and Zn(II)

The time necessary to reach the equilibrium of adsorption of Hg(II) and Zn(II)onto (GAC_8) was investigated at initial concentration of 80 mg/L. The effect of contact time (from 0 to 120 min) on the adsorption of Hg(II) and Zn(II)metal ions is presented in Fig.5. The evolution of the adsorbed amount of metal ions with the contact time indicates that the equilibrium was relatively fast and was totally reached in about 90 min for the metal ions. In Fig.5, two kinetic regions can

be observed: the first one is characterized by a high adsorption rate and this is due to the fact that initially the number of sites of available activated carbon is higher and the driving force for mass transfer is greater. Metal ions easily access first the adsorption sites. As time progresses, the number of GAC_8 free sites decreases and the non-adsorbed cations in solution are assembled on the surface, thus limiting adsorption capacity.

3.2.2. Equilibrium isotherms

The capacity of a GAC can be described by equilibrium sorption isotherm, which is characterized by certain constants whose values express the surface properties and affinity of the GAC. The adsorption isotherms were investigated using three equilibrium models, namely: the Freundlich, Langmuir and Temkin isotherm models.

The Langmuir sorption isotherm has been successfully applied to many pollutant biosorption processes and has been the most widely used isotherm for the biosorption of a solute from a liquid solution [13]. A basic assumption of the Langmuir theory is that sorption takes place at homogeneous sites within the sorbent. This model can be written in a linear form [7].

$$\frac{C_e}{q_e} = \frac{1}{K_L q_{\max}} + \frac{1}{q_{\max}} C_e \quad (1)$$

Where q_e(mg/g) is the equilibrium adsorption amount on the adsorbent, C_e (mg/L) is the equilibrium metal ion concentration, q_{max} (mg/g) is the maximum adsorption capacity, and K_L (L/mg) is the monolayer adsorption capacity of the Langmuir adsorption constant related with the free energy of adsorption. Fig.5 indicates the linear relationship between the amount (mg) of Hg(II) and Zn(II) ions sorbed per unit mass (g) of activated carbons derived from Theobroma cacao pod husk against the concentration of Hg(II) and Zn(II) ions remaining in solution (mg/L). The coefficients of correlation (R^2) were found to be 0.970 and 0.997 for Hg(II) and Zn(II) adsorption, respectively. These results indicate that the adsorption of the metal ions onto activated carbons derived from Theobroma cacao pod husk fitted well the Langmuir model. In other words, the sorption of Hg(II) and Zn(II) ions onto activated carbons derived from Theobroma cacao pod husk was taken place at the functional groups/binding sites on the surface of the GAC which is regarded as monolayer biosorption. The K_L value was found as 0.029 L/mg for Hg(II) ion and 0.007 L/mg for Zn(II) ion.

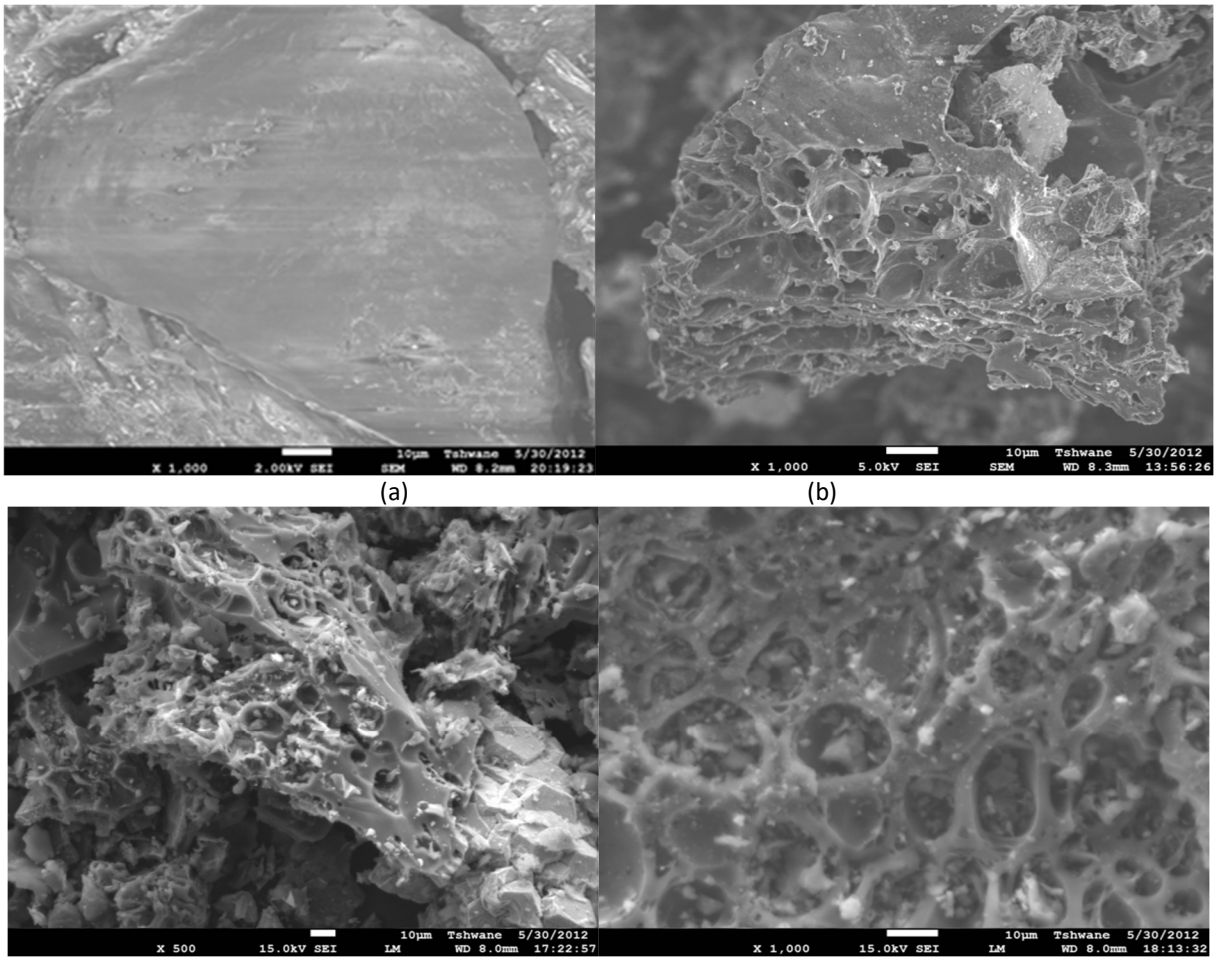

(a) (b)

(c) (d)

Fig.4*. SEM images of GAC_0 (a), GAC_1 (b), GAC_7 (c) and GAC_8 (d).*

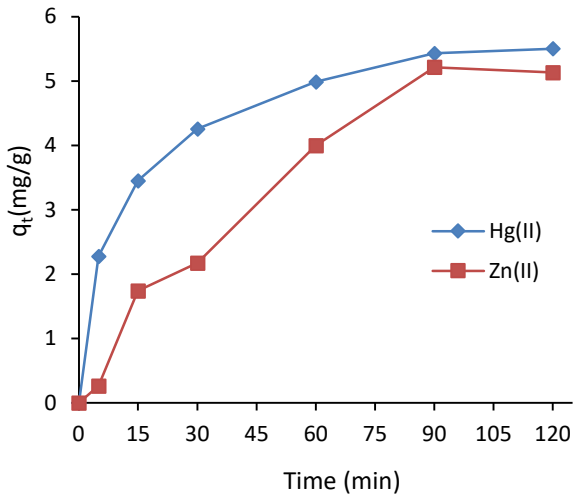

Fig.5.*Kinetic curves of contact time on Hg(II) and Zn(II) adsorption onto GAC₈ from an aqueous solution*

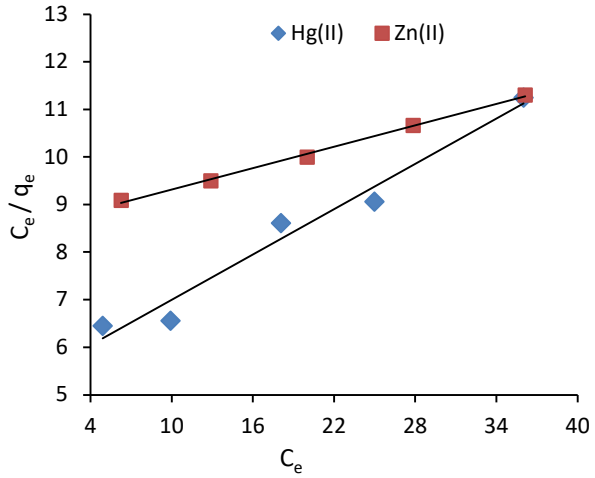

Fig.6*. Langmuir adsorption isotherm for removal of Hg(II) and Zn(II) onto GAC₈ at room temperature.*

The Freundlich model assumes a heterogeneous adsorption surface and active sites with different energy. The model can be expressed as [29]:

$$\log\left(\frac{x}{m}\right) = \log K_F + \frac{1}{n}\log C_e \qquad (2)$$

where K_F (mg/L)(L/g)$^{1/n}$is a constant relating the adsorption capacity and 1/*n* is a constant depicting the adsorption intensity, which varies with the heterogeneity of the material (Fig.7). The values of $K_F$and 1/*n* were found to be 1.323 and 0.583 for Hg(II) adsorption and 0.426 and 0.878 for Zn(II) adsorption. The 1/*n* values were between 0 and 1 indicating that the adsorption of Hg(II) and Zn(II) onto activated carbons derived from *Theobroma cacao* pod huskwas favorable. However, the R^2values were found to be 0.892 for Hg(II) adsorption and 0.998 for Zn (II) adsorption. These results indicate that the Freundlich model was not able to adequately to describe the relationship between the amounts of sorbed metal ions and their equilibrium concentration in the solution for Hg(II) but fitted well for Zn(II).

The Temkin isotherm contains a factor that explicitly takes into account of the adsorbent-adsorbate interactions. In this equation, it is assumed that, because of these interactions and ignoring very low and very large concentration values, the heat of adsorption of all molecules in the layer would decrease linearly with the coverage [29]. The Temkin model is written as:

$$q_e = B \ln A_T + B \ln Ce \qquad (3)$$

The parameters calculated from Temkin's linear model (Fig.8) are: A_T = 0.639L/gfor Hg(II), A_T = 0.529L/g for Zn(II) and B = 2.816 kJ/mol for Hg(II), B = 3.247 kJ/mol for Zn(II), indicating that the adsorption of Hg(II) and Zn(II) onto activated carbons derived from *Theobroma cacao* pod husk occurred via physisorption. The constant B in Temkin isotherms are less than 8 kJ/mol, so the mechanism involved is physical adsorption. In the physisorption process, the adsorbates adhere to the adsorbent through a weak Van Der Waals interactions and thus this process is associated with relatively low adsorption energies [30].

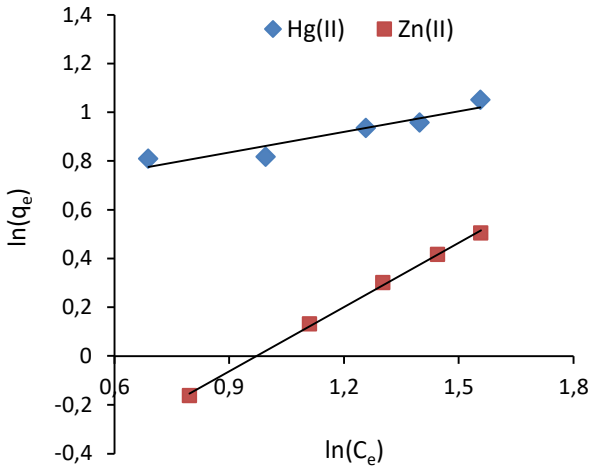

Fig.7*. Freundlich adsorption isotherm for removal of Hg(II) and Zn(II) onto GAC₈ at room temperature.*

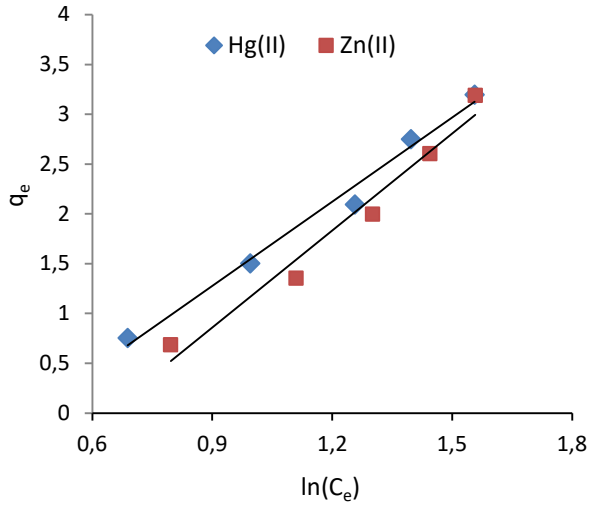

Fig.8*.Temkin adsorption isotherm for removal of Hg(II) and Zn(II) onto GAC₈ at room temperature.*

3.3 Kinetic Studies

Kinetic study of process is necessary to obtain information about the adsorption mechanism, which is crucial for the practicality of the process. The mechanism of the adsorption process depends on the physical and chemical characteristic of the adsorbent and adsorbate.

3.3.1 Pseudo-first order model

The pseudo-first order rate equation was proposed by Lagergren and is widely used for the adsorption of liquid/solid system [31]. The linear form of Pseudo-first orderequation is expressed as:

$$\log(q_e - q_t) = \log q_e - \frac{k_1 t}{2.303} \quad (4)$$

Where k_1 (min^{-1}) is the rate constant of pseudo-first order equation. q_e and q_t are the adsorption capacity at equilibrium and at time t(min), respectively. Slope and intercept of the straight line plot $log(q_e–q_t)$ vs t give the values of k_1 and q_e respectively. The pseudo-first order plots for Hg(II) and Zn(II) are shown in Fig.8. The values of k_1 for Hg(II) and Zn(II) obtained from the straight line plot were 0.040 and 0.028 min^{-1}, respectively. The values of regression coefficients (Table 2) were 0.970 and 0.985, which suggested that plots for Hg(II) and Zn(II) were linear over a wide range of initial concentrations. Therefore, pseudo-first order kinetic model described well Hg(II) and Zn(II) onto activated carbons derived from *Theobroma cacao* pod husk.

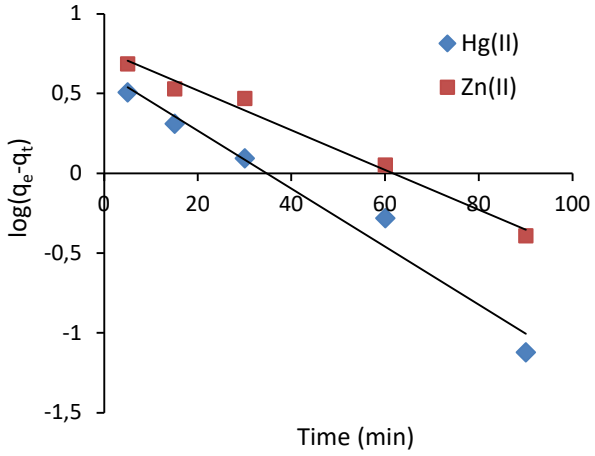

***Fig.8**. Pseudo-first order kinetic plots for Hg(II) and Zn(II) onto GAC_8 at room temperature.*

3.3.2. Pseudo-second order model

The metal species are held at appropriate ion-exchange sites on the surface by chemical bond formation. Pseudo-second order model [32,33] suggests that both number of adsorption sites on the material surface and concentration of adsorbate ions in the liquid phase determine the rate. The linear form is:

$$\left(\frac{t}{q_t}\right) = \left(\frac{t}{q_e}\right) + \left[\left(\frac{1}{k_2 q_e^2}\right)\right] \quad (5)$$

where $h = k_2 q_e^2$ and k_2 are initial and overall rate constants for adsorption which can be calculated from slope and intercept of plot t/q_t vs t. Pseudo-second order plots for Hg(II) and Zn(II) are shown in Fig.9. k_2 for Hg(II) adsorption was found to be 0.016 mg/g·min and smaller than initial rate constant, h = 0.575 mg/g·min. This showed that the rate of Hg(II) adsorption was much faster at the beginning and slowed down with the passage of time. The regression coefficient values (Table 2) for Hg(II) and Zn(II) were 0.998 and 0.975, which indicated a better suitability of pseudo-second order kinetics in the adsorption process, as compared to pseudo-first order model. Thus Hg(II) adsorption followed pseudo-second order kinetics, whereas Zn(II) adsorption followed partially pseudo-first order and pseudo-second order kinetics [34,35].

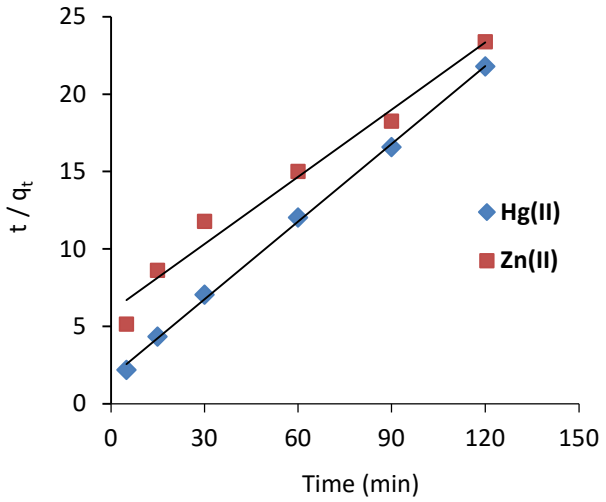

***Fig.9**. Pseudo-second order kinetic plots for Hg(II) and Zn(II) onto GAC_8 at room temperature.*

Table 2
Kinetics parameters for Hg(II) and Zn(II) adsorption onto *Theobroma cacao* pod husk activated carbons.

Model	Lagergren		Pseudo second order			Intra-particle Diffusion		Elovich kinetic model		
	k_1 (min^{-1})	R^2	k_2 (g/mg.min)	R^2	h (mg/g.min)	K_w ($mg/gmin^{0.5}$)	R^2	β	α	R^2
Hg(II)	0.040	0.970	0.006	0.975	0.167	1.384	0.956	0.950	1.853	0.995
Zn(II)	0.028	0.985	0.016	0.998	0.571	0.089	0.923	0.622	0.673	0.990

3.3.3. Elovich kinetic model

Elovich kinetic relationship, developed by is suitable to describe second order kinetics assuming that the solid surfaces are energetically heterogeneous. Thus, the model describes the rate of chemical adsorption on energetically heterogeneous surface [30,36]. The mathematical relationship in linearized form is:

$$q_t = 1/\beta \ln(\alpha\beta) + 1/\beta \ln t \quad (6)$$

where α is the initial adsorption rate (mg/g·min) and β (g/mg) is the desorption constant during any one experiment. The initial adsorption rate α and the desorption constant β were calculated from slope and intercept of straight line plot between q_t and *ln(t)* for Hg(II) and Zn(II) (Fig.10). α value for Hg(II) was found to be 1.895 mg/g·min, which was greater than β value (0.950 g/mg); therefore, the rate of adsorption was much higher than the rate of desorption. This showed the viability of adsorption process. On the other hand, for Zn(II), *α*value was 0.673 mg/g.min, which was higher than β (0.622 g/mg); therefore, the rate of adsorption was again much smaller than desorption. Thus α and β values showed the viability of Hg(II) and Zn(II) adsorption onto GAC_8. High regression coefficients of 0.995 and 0.990 (Table 3) for Hg(II) and Zn(II) indicated well fitting of adsorption data to Elovich kinetic model.

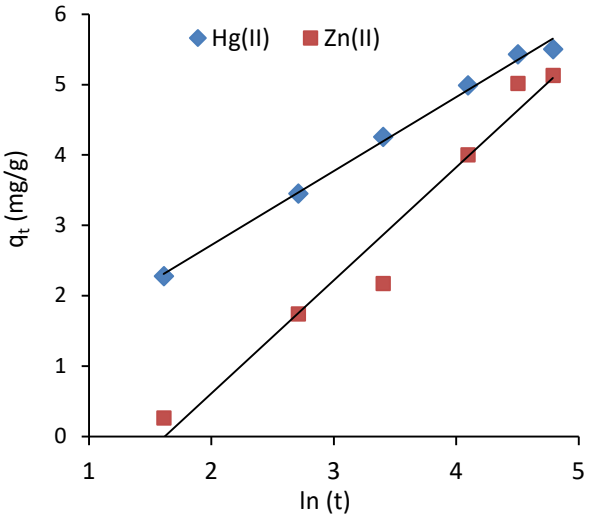

Fig.10*.Elovich kinetic plots for Hg(II) and Zn(II) onto GAC_8 at room temperature.*

3.3.4. Intra-particle diffusion

Once adsorbed on the surface, solute particles diffuse into the pores on the surface of adsorbent and form bonding, which may be the rate determining step [37,38]. Weber and Morris intra-particle diffusion model is given:

$$q = f\left(\frac{D_t}{r_p^2}\right)^{1/2} = k_w t^{1/2} \quad (7)$$

where k_w (mg/g·min$^{1/2}$) is the rate constant for intra-particle diffusion.k_w can be found from slope of plot lnq_t vs ln*t*. For an adsorbing system the straight line should pass through the origin and the intercept value provides an idea about the deviation from intra-particle diffusion model or contribution of the film diffusion mechanism [37-39]. k_w for Hg(II) and Zn(II) adsorption were observed to be 1.384 and 0.089 mg/g.min$^{1/2}$ (Fig.11). The regression coefficients for Hg(II) and Zn(II) were 0.956 and 0.923; therefore, plots were straight line but did not pass through the origin and had intercepts 0.325 and -2.417, which suggested that adsorption of Hg(II) and Zn(II) did not depend on intra-particle diffusion step. The intra-particle process depends on the size of the particle to be adsorbed and size of the pores on the surface of adsorbent. Therefore, in the present case, size of Hg(II) and Zn(II) ions should be larger than the size of pores on the adsorbent.

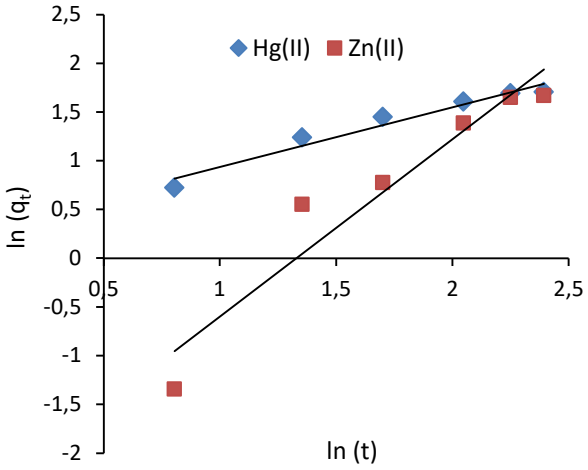

Fig.11*. Intra-particle diffusion plots for Hg(II) and Zn(II) onto GAC_8 at room temperature.*

4. Conclusion

The aim of this work was to investigate the removal of Hg(II) and Zn(II) ions from aqueous solutions by using activated carbons derived from lowland bioresource material (*Theobroma cacao* pod husk). Optimal removal conditions for both metals were determined with batch experiments. Simultaneous adsorption of Hg(II) and Zn(II) ions reached equilibrium faster (within 90 min.). Experimental results were evaluated with Langmuir, Freundich and Temkin isotherms. In addition to higher values of correlation coefficients, monolayer capacities (*V*) determined from Langmuir isotherm and adsorption intensities (*n*) determined from Freundlich isotherm indicate appropriateness of Langmuir and Freundlich isotherms for both metals. In Temkin isotherm, it was stated that adsorbate/adsorbate interactions are weaker for zinc removal due to smaller values of Temkin constant (*A*). Pseudo-first-order, pseudo-second-order and Elovich model reaction kinetic has provided a realistic description for removal of Hg(II) and Zn(II).

Conflicts of interest

The authors declare no conflicts of interests.

References

[1] S.S. Ahluwalia, D. Goyal, Microbial and plant derived biomass for removal of heavy metals from wastewater, Bioresource Technology 98 (2007) 2243–2257.

[2] A. Kirby, I. Rucevska, V. Yemelin, C. Cooke, O. Simonett, V. Novikov, G. Hughes, UNEP Global Mercury Assessment: Sources, Emissions, Releases and Environmental Transport, United Nations Environment Protection (UNEP), Report, 2013.

[3] Pollution Prevention and Abatement Handbook WORLD BANK GROUP Effective July, 1998.

[4] S. Wang, X. Shi, Molecular mechanism of metal toxicity and carcinogenesis,Molecular and Cellular Biochemistry222(2001) 3–9.

[5] U.S. EPA (U.S. Environmental Protection Agency). http://www.epa.gov/mercury/ [accessed 10 October 2013].

[6] C.M. Kede, M.A. Etoh, P.P. Ndibewu, H.M. Ngomo, P.M. Ghogomu, Equilibria and kinetic studies on the adsorption of cadmium onto Cameroonian wetland clays. British Journal of Applied Science & Technology 4(7) (2014) 1070-1088.

[7] E. Igberase, P. Osifo, A. Ofomaja, The adsorption of copper (II) ions by polyaniline grafted chitosan beads from aqueous solution: equilibrium, kinetic and desorption studies, Journal of Environmental Chemical Engineering 2(2014) 362–369.

[8] D. Mohan, P.K. Singh, Single and multi-component adsorption of cadmium and zinc using activated carbon derived from bagasse an agricultural waste Water. Research 36 (2002) 2304–2318.

[9] V.K. Gupta, A. Rastogi, A. Nayak, Adsorption studies on the removal of hexavalent chromium from aqueous solution using a low cost fertilizer industry waste material,Journal of Colloid and Interface Science342 (2010) 783–842.

[10] T. Viraraghavan, A. Kapoor, Adsorption of mercury from wastewater by bentonite, Applied Clay Science 9(1994) 31-49.

[11] S. Kushwaha, G. Sreelatha, P. Padmaja, Physical and chemical modified forms of palm shell: preparation, characterization and preliminary assessment as adsorbents, Journal of Porous Materials 20 (2013) 21–36.

[12] M. Eloussaief, A. Sdiri, M. Benzina, Modelling the adsorption of mercury onto natural and aluminium pillared clays, Environmental Science and Pollution Research 20 (2013) 469–479.

[13] W.T. Tsia, H.R. Chen, Removal of malachite green from aqueous solution using low-cost chlorella based biomass,Journal of Hazardous Materials 175 (2010) 844–849.

[14] I. Langmuir, The adsorption of gases on plane surfaces of glass, mica and platinum, Journal of the American Chemical Society 40 (1918) 1361–403.

[15] A.H. Azizah, N.M. Nik Ruslawati, T.T. Swee, Extraction and characterization of antioxidant from cocoa by-products. Food Chemistry 64 (1999) 199–202.

[16] R. Redgwell, V. Trovato, S. Merinat, D. Curti, S. Hediger, Dietary fibre in cocoa shell: characterisation of component polysaccharides, Food Chemistry 81(2003)103–112.

[17] E. Aregheore, Chemical evaluation and digestibility of Cocoa (Theobroma cacao) by products fed to goats,Tropical Animal Health and Production 34(2002) 339–348.

[18] O Adeyi, Proximate composition of some agricultural wastes in Nigeria and their potential use in activated carbon production, Journal of Applied Sciences and Environmental Management 14 (2010) 55-58.

[19] K. Kadirvelu, M. Kavipriya, C. Karthika, M. Radhika, N. Vennilamani, S. Pattabhi, Utilization of various agricultural wastes for activated carbon preparation and application for the removal of dyes and metal ions from aqueous solutions, Bioresource Technology 87 (2003) 129–132.

[20] A. Basu, M.S. Rahaman, S. Mustafiz, M.R. Islam, Batch studies of lead adsorption from a multi-component aqueous solution onto Atlantic cod fish scale (Gadusmorhua) substrate, Journal of Environmental Engineering and Science 6 (2007) 455–462.

[21] N. Barka, M. Abdennouri, M. El Makhfouk, S. Qourzal, Biosorption characteristics of cadmium and lead onto eco-friendly dried cactus (opuntia ficus indica) cladodes, Journal of Environmental Chemical Engineering 1(2013); 144–9.

[22] N. Barka, S. Qourzal, A. Assabbane, A. Nounah, Y. Ait-Ichou, Removal of reactive yellow 84 from aqueous solutions by adsorption onto hydroxyapatite, Journal of the Saudi Chemical Society 15 (2011) 263–267.

[23] C.M. Kede, P.P. Ndibewu, Makonga M. Kalumba, Nikolay A. Panichev, M. Ngomo, J.M. Ketcha, Adsorption of Mercury (II) onto Activated Carbons derived from Theobroma cacao Pod Husk, South African journal of chemistry 68 (2015) 226-235.

[24] A. Bhatnagara, M. Sillanpää, Utilization of agro-industrial and municipal waste materials as potential adsorbents for water treatment. A review, Chemical Engineering Journal 157 (2010) 277–296.

[25] Z. Chen, W. Ma, M. Han, Biosorption of nickel and copper onto treated alga (undariapinnarlifida): application of isotherm and kinetic models, Journal of Hazardous Materials 155 (2008) 327–333.

[26] T.S. Anirudan, P.G. Radhakrishnan, Thermodynamics and kinetics of adsorption of Cu(II) from aqueous solution onto a new cation exchanger derived from tamarind fruit shell,The Journal of Chemical Thermodynamics 40(2008) 702–709.

[27] R.C. Bansal, G. Meenakshi, Activated carbon adsorption, CRC Press. (2005) 85-91.

[28] J.C.P. Vaghetti, E.C. Lima, B. Roger, J.L. Brasil, B.M. Da Cunha, N.M. Simon, N.F. Cardoso, C.P. Zapata Noreña, Application of Brazilian-pine fruit coat as a biosorbent for removal of Cr(VI) from aqueous solution-kinetic and equilibrium study, Biochemical Engineering Journal 42 (2008) 67–76.

[29] S. Lagergren, ZurTheorie der Sogenannten Adsorption GelösterStoffe," Kungliga Svenska Vetenskapsakademiens. Handlingar, 24(4) (1898) 1–39.

[30] Y.S. Ho, G. McKay, Pseudo-second-order Model for Sorption Processes, Process Biochemistry 34 (1999) 451–465.

[31] S. Vafakhah, M.E. Bahrololoom, R. Bazarganlari, M. Saeedikhani, Removal of copper ions from electroplating effluent solutions with native corn cob and corn stalk and chemically modified corn stalk, Journal of Environmental Chemical Engineering 2(2014) 356–361.

[32] M. Imamoglu, O. Tekir, Removal of copper (II) and lead (II) ions from aqueous solution by adsorption on activated carbon from a new precursor hazelnut husks, Desalination 228(2008) 108–113.
[33] V.T.P. Vinod, R.B. Sashidhar, A.A. Sukumar, Competitive adsorption of toxic heavy metal contaminants by gumkondagogu: a natural hydrocolloid, Colloids and surfaces B: Biointerfaces 75(2010) 490–502.
[34] M. Ghaedi, A. Ansari, M.H. Habibi, A.R. Asghari, Removal of malachite green from aqueous solution by zinc oxide nanoparticles loaded on activated carbon: kinetics and isotherm study, Journal of Industrial and Engineering Chemistry 20(2014) 17–28.
[35] M. Ghaedi, HZ. Khafri, A. Asfaram, A. Goudarzi, Response surface methodology approach for optimization of adsorption of janus Green B from aqueous solution onto ZnO/Zn(OH)2-NP-AC: kinetic and isotherm study, Spectrochimica Acta Part A: Molecular and Biomolecular Spectroscopy 152 (2016) 233-240.
[36] H. Mazaheri, M. Ghaedi, S. Hajati, K. Dashtian, M.K. Purkait, Simultaneous removal of methylene blue and Pb^{+2} ions using ruthenium nanoparticle-loaded activated carbon: response surface methodology, RSC Advances 5 (2015) 27–35.
[37] M. Jamshidi, M. Gaedi, K. Dashtian, S. Hajati, A.A. Bazrafshan, Sonochemical assisted hydrothermal synthesis of ZnO: Cr nanoparticles loaded activated carbons for simultaneous ultrasound-assisted adsorption of ternary toxic organic dye: derivative spectrophotometric, optimization, kinetic and isotherm study, Ultrasonics Sonochemistry 32 (2016) 119–131.
[38] A. Asfaram, M. Ghaedi, S. Hajati, A. Goudarzi, A.A. Bazrafshan, Simultaneous ultrasound-assisted ternary adsorption of dyes onto copper-doped zinc sulphide nanoparticles loaded on activated carbon: optimization by response surface methodology, Spectrochimica Acta Part A: Molecular and Biomolecular Spectroscopy 145(2015) 203–212.
[39] Y. Zhu, J. Hu, J. Wang, competitive adsorption of Pb(II), Cu(II) and Zn(II) onto xanthate-modified magnetic chitosan, Journal of Hazardous Materials 221-222(2012) 155–161.